PROCEEDINGS OF SPIE

SPIEDigitalLibrary.org/conference-proceedings-of-spie

A UV double pass spectrograph for monitoring stellar activity for the Keck Planet Finder

Ashley Baker, Steven Gibson, Jason Grillo, Yuzo Ishikawa, Andrew Howard, et al.

Ashley D. Baker, Steven R. Gibson, Jason Grillo, Yuzo Ishikawa, Andrew Howard, Samuel Halverson, Kodi Rider, Sharon Jelinsky, William Deich, Martin M. Sirk, Howard Isaacson, Arpita Roy, Jerry Edelstein, Christopher Smith, "A UV double pass spectrograph for monitoring stellar activity for the Keck Planet Finder," Proc. SPIE 12184, Ground-based and Airborne Instrumentation for Astronomy IX, 121845H (29 August 2022); doi: 10.1117/12.2628149

SPIE.

Event: SPIE Astronomical Telescopes + Instrumentation, 2022, Montréal, Québec, Canada

A UV Double Pass Spectrograph for Monitoring Stellar Acitivity for the Keck Planet Finder

Ashley D. Baker[a], Steven R. Gibson[a], Jason Grillo[b], Yuzo Ishikawa[c], Andrew Howard[a], Samuel Halverson[d], Kodi Rider[b,e], Sharon Jelinsky[b,f], William Deich[g], Martin M. Sirk[b], Howard Isaacson[e], Arpita Roy[h], Jerry Edelstein[b], and Christopher Smith[b]

[a]California Institute of Technology, Pasadena, United States
[b]Space Sciences Laboratory, Berkeley, CA, United States
[c]Johns Hopkins University, Baltimore, MD, United States
[d]Jet Propulsion Laboratory, California Institute of Technology, Pasadena, CA, United States
[e]University of California, Berkeley, CA, United States
[f]Lawrence Livermore National Lab, Berkeley, CA United States
[g]University of California, Santa Cruz, CA United States
[h]Space Telescope Sciences Institute, Baltimore, MD, United States

ABSTRACT

We present a compact, double-pass cross-dispersed echelle spectrograph that is tailored specifically to cover the 383 nm to 403 nm spectral range and record R∼16,000 spectra of the stellar chromospheric Ca II H&K lines. This 'H&K' spectrometer was developed as a subsystem of the Keck Planet Finder (KPF), which is an extremely precise optical (440 - 870 nm) radial velocity spectrograph for Keck I, scheduled for commissioning Fall 2022, with the science objective of measuring precise masses of exoplanets. The H&K spectrometer will observe simultaneously with KPF to independently track the chromospheric activity of the host stars that KPF observes, which is expected to dominate the KPF measurement floor over long timescales. The H&K Spectrometer is fiber-fed from the KPF fiber injection unit with total throughput of 4-7% (top of telescope to CCD) over its operating spectral range. Here we detail the optical design trade offs, mechanical design, and first results from alignment and integration testing.

Keywords: Spectrographs, Stellar Activity, Radial Velocity Surveys

1. INTRODUCTION

The Keck Planet Finder (KPF) is a next generation extremely precise radial velocity (RV) spectrograph that is scheduled for delivery to Keck I at W.M. Keck Observatory (WMKO) in late Fall 2022.[1,2] One of the benefits of KPF is its high throughput over its spectral range spanning from 440 nm to 870 nm. The RV precision goal for KPF is ∼30 cm s^{-1}, and it will measure precise RVs for stars as faint as V∼15 mag.

One of the primary challenges that KPF and other exoplanet RV surveys face is stellar activity, which can add RV signals that can hide or mimic an exoplanet RV signal.[3,4] To combat this, RV surveys often track the activity of the host star by measuring the flux in the core of key stellar lines relative to a nearby continuum region.[5,6] The Ca II H line at 3968.469 Å the Ca II K line at 3933.663 Å (vacuum) were the first activity indicators to be widely observed[7] and are still a commonly used metric for measuring chromospheric stellar activity.[3,8] The S_{HK} index was developed by O.C. Wilson, who first observed the correlation between the Ca II H&K line cores and activity in the chromosphere. For a given flux value in the cores of the Ca II H&K lines, N_H and N_K, an activity index can be computed by comparing these values to the flux in nearby continuum regions (N_V and N_R). The activity index, S_{HK}, is then defined as:

Further author information: (Send correspondence to A.D.B.)
A.D.B.: E-mail: abaker@caltech.edu

Ground-based and Airborne Instrumentation for Astronomy IX, edited by Christopher J. Evans, Julia J. Bryant, Kentaro Motohara, Proc. of SPIE Vol. 12184, 121845H
 · 0277-786X · doi: 10.1117/12.2628149

$$S_{HK} = \alpha \frac{N_H + N_K}{N_V + N_R} \quad (1)$$

Here, α accounts for instrument-specific normalizations, so that S_{HK} values can be compared between instruments.

To cover the spectral region of the Ca II H&K lines, KPF will utilize a separate spectrometer called the "H&K spectrometer" that will collect light simultaneously with the main instrument during KPF exposures in order to measure stellar activity using the Ca II H&K lines. The H&K spectrometer was chosen to have a cross-dispersed echelle design in a double-pass setup (i.e. the camera and collimator are one in the same). The design, integration, and performance verification are described in the following sections.

As RV instruments extend into near infrared (NIR) wavelengths, where spectral line activity indicators are not as well studied,[6] stand alone activity monitoring instruments may become more common. In the case of KPF, a separate near-UV spectrometer with more relaxed requirements significantly eased the optical design complexity of the main instrument, as the 'parent' spectrometer no longer needed to extend blueward of 400 nm (where there is minimal effective stellar information content for the majority of KPF target stars). This allowed for a more streamlined optical design with higher-efficiency coatings and smaller detectors.

2. REQUIREMENTS

The goal of KPF's H&K spectrometer is to provide precise activity indices simultaneously with the main instrument. For each KPF exposure there should be at least one exposure taken with the H&K and therefore at least one measurement of S_{HK}. The time series of the extracted S_{HK} values must be precise enough to reveal stellar activity signatures that can then be correlated with RVs. To determine the throughput and resolution requirements for the H&K spectrometer, we used the typical RMS of the S_{HK} indices measured by HIRES on a variety of classical RV target stars as a benchmark.[8,9] HIRES achieves a typical performance of 0.002 (RMS of S_{HK} on bright target). For KPF, we impose a performance goal of half of this value: $\sigma_{S_{HK}} < 0.001$.

Work to constrain the instrument requirements, including the resolution, throughput (telescope to detector, inclusive) and read noise was completed in a study by Ishikawa et al. (in prep). In this analysis by Ishikawa et al., HIRES[9] (R∼70,000) time series spectra of two active stars were degraded to lower resolutions. Read noise and photon noise was added corresponding to a respective throughput and the assumption of an exposure time such that the observation length would result in the main KPF spectrometer reaching its nominal target SNR of 70. This transformation was performed for each HIRES spectrum and then the S_{HK} index, calculated as shown in Equation 1, was derived and compared to the extracted S_{HK} indices derived from the original high resolution dataset. Ishikawa et al. then compared the RMS of the difference between the S_{HK} values extracted from the original high resolution dataset and that of degraded dataset for a grid of resolutions, read noise values, throughputs, and pixel samplings. The combination of parameter values that meet the science goal of $\sigma_{S_{HK}} < 0.001$ are summarized in Table 1 along with the corresponding values of the final optical design.

A few comments on the requirements listed in Table 1:

- The two fibers correspond to a science trace and sky trace that are illuminated by the KPF Fiber Injection Unit (FIU), which is described in Ref. 10.
- The throughput requirement led to the installation of the H&K spectrometer within a rack in the Keck Adaptive Optics (AO) room. This allowed for the shortest possible fiber lengths and minimized UV attenuation within the fibers.
- The spectral stability requirement was set to simplify the spectral extraction pipeline and to ensure the orders do not shift too close to the edge of the detector.

Table 1. Requirements for KPF's Ca II H&K spectrometer along with the corresponding values for the final design.

Parameter	**Requirement**	**Designed**
Bandpass	Orders covering Ca II H&K features plus adjacent orders	383 nm-402 nm
Resolving Power	14,000 - 17,000	16,000
Sampling	3-5 pix	4 pix
Throughput	$> 4\%$	4% - 7%
Read Noise	< 8 e-	5.8 e-
Sky Subtraction	Simultaneous science and sky spectra	Interleaved echelle spectra from 225 μm Science and Sky fibers
Inter-order Separation	> 4 pix	5-7 pix
Spectral Stability	< 1 pix movement	< 1 pix

3. OPTICAL DESIGN

An overview of the H&K spectrometer design is shown in Figure 1. The core design centers around a double-pass, all-refractive camera with a R4 primary disperser and VPH cross-disperser. The input is a set of 225 um fibers, injected at the KPF Fiber Injection Unit, which pass through a set of pre-optics leading up to a spectral slit. The final spectra are recorded on a commercial Andor CCD package. The final throughput of the design is shown in Figure 2 (left) and is broken down by section of the optical path (right).

3.1 VPH vs. Cross Dispersed Trade Off

A trade study was performed comparing a design with a VPH as the only dispersing element to a different cross dispersed echelle spectrograph design, the latter of which was ultimately chosen. Considering the 10 m aperture of Keck I and the 225 μm fiber sizes, the throughput, cost, size and design complexity were compared for each of the two designs. The downsides of the VPH-only design included losses due to a smaller slit width (the alternative of increasing the collimated beam diameter was also not preferred due to size constraints), the added cost of a wider 2k detector, and the large angle of incidence on the VPH. Cost and size were comparable to the two designs, and while the double pass design has slightly more added complexity due to mounting the echelle, we estimated a higher throughput for the cross-dispersed echelle design.

3.2 Component Choices

3.2.1 Echelle

The echelle is an R4 grating fabricated on a Zerodur substrate, produced by Richardson Grating with a groove density of 31.6 grooves/mm and an aluminum coating with a second coating layer of MgF_2 to protect from oxidization over its lifetime. The MgF_2 layer decreases the overall throughput by a factor of 5-6%, but should prevent a buildup of Al_2O_3 over time as observed by Ref. 11. The grating dimensions are 220 mm (length) by 70 mm (width), by 35 mm (thickness). The designed 2 degree gamma angle allows the beam to pass back through the cross disperser and camera/collimator and form an image on the detector without clipping the fold mirror at the input relay.

3.2.2 Camera/Collimator

Because the beam passes twice through the camera/collimator optics along slightly different axes due to the grating gamma angle, the lenses had to be uniquely optimized to meet the optical resolution requirements accross the bandpass. An initial throughput study of the complete optical design showed that a camera/collimator made of CaF_2, the initial glass choice mentioned in Ref. 2, would not be sufficient for meeting the instrument throughput requirements, though it offered good optical performance. A singlet and doublet lens combination using the glasses PBM2Y and S-FSL5Y offered the best image quality for the fewest number of lenses and the

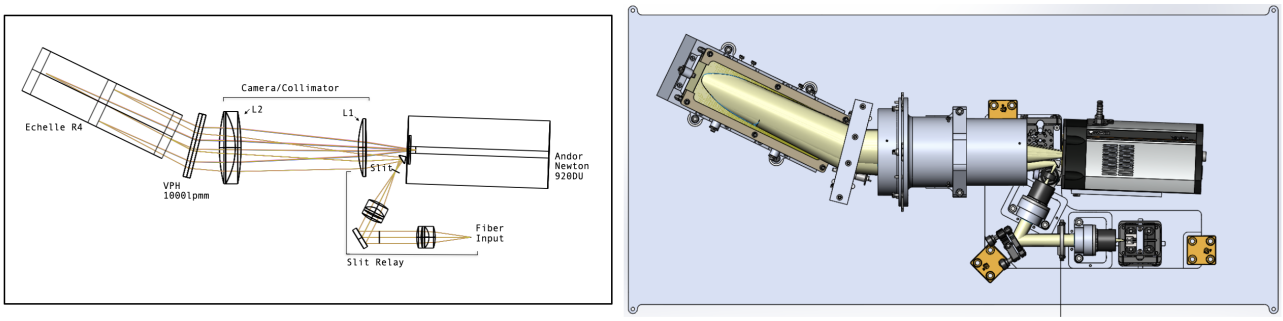

Figure 1. The optical design of the H&K spectrometer (left) and the mechanical design of the optical mounts (right).

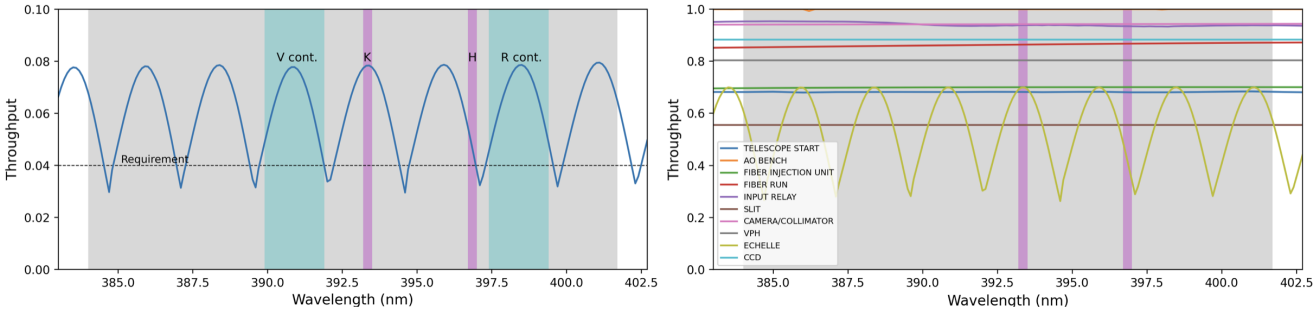

Figure 2. Total throughput of the H&K spectrometer (left) and the transmission of various optical paths in the system (right). Fiber coupling losses due to seeing are included in the FIU path (estimated to be 72% based on nominal seeing conditions of 0.7 arcsec FWHM). Telescope reflectivity was based on 2019 coating curves for Keck 1 with an additional 2% degradation to account for the coating age. The echelle blaze profile shown here differs from that of the actual H&K echelle due to a difference in blaze angle from the originally assumed R4, which is assumed here.

highest throughput over the instrument's bandpass. A test plate fitting in Zemax was performed to match the lens radii to test plates available to the vendor, Optimax*.

3.2.3 Fiber Input and Relay

The input optical fibers are 225 μm octagonal core, which are identical to the primary KPF science fibers but are coated with a UV-optimized anti-reflection (AR) coating. The optical design was optimized for three fiber inputs: the required science and sky fibers for night time observing, and a third day-time fiber to be illuminated with solar light. Only science and sky fibers were installed in the v-groove plate that holds to fibers to illuminate the instrument, but the third fiber may be included in the future†. Because of the constrained 1:1 magnification of the system and target 4 pixel sampling, a 104 μm width slit needed to be applied to the fibers. To avoid the risk of damaging the fiber tips or their AR coating by applying a slit directly to the fiber tips, we opted to re-image the fibers onto a slit mask using a telecentric relay. This also provided a pupil plane for positioning a pupil stop and a place for positioning the mechanical shutter.

The optimal fiber-to-fiber spacing was determined to 0.45 mm, which was balanced with the VPH line density to achieve >4 pixels of space between orders. This small inter-fiber distance drove the choice to use a v-groove plate to mount the fibers, which is discussed further in §4. The design of the lenses for the relay were copied from a lens designed for the H&K arm of the KPF Fiber Injection Unit (FIU). Custom lenses were chosen over

*https://www.optimaxsi.com/

†Solar light can also be passed through the calibration arm of KPF's FIU, but the optical coatings were not optimized for the H&K bandpass so 30 min exposure times would be required and are unlikely to be feasible. However, the throughput is still high enough that if a solar fiber is installed, a blocking filter may need to be added in the calibration light path to prevent light from entering the science and sky traces, which overlap the solar order trace.

several less expensive off-the-shelf (OTS) lenses we investigated because they offered superior optical quality that minimized slit losses and preserved good image quality (<26 μm spot RMS) in the final spectrum.

The slit relay was folded with an OTS mirror to fit in a 1 ftx3 ft optical bench footprint. The slit mask was purchased through National Aperture[‡] and the rectangular slits were rotated in order to compensate for the echelle gamma angle that cause line shearing of the resolution element. The CCD was also clocked to straighten the orders with respect to the pixel grid and the combined effect of this and the slit rotation is demonstrated in Figure 3. A final slit rotation of 20 degrees resulted in resolution elements with edges aligned to the pixel grid. When installing the fibers in the v-groove mount, they were rotated 20 deg to match the slit rotation; this put the edges of the octagon aligned to the slit, which reduced slit losses by ∼0.2%.

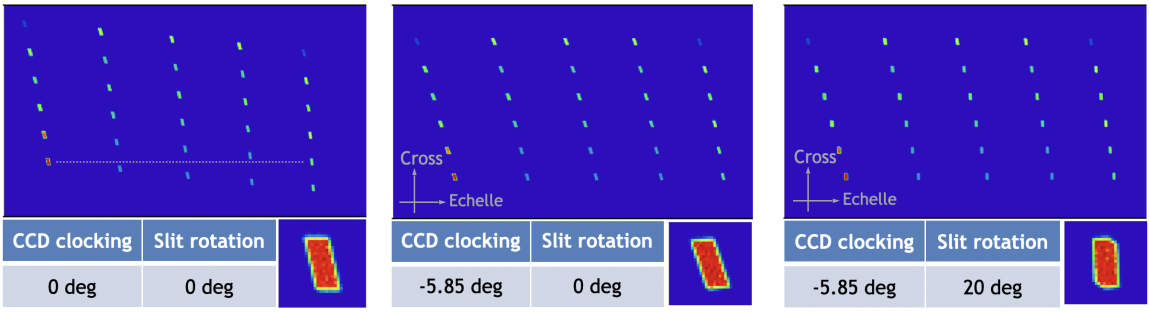

Figure 3. Demonstration of clocking the CCD and rotating the slit in order to produce orders and resolution elements in line with the pixel grid in order to simplify the spectral extraction procedure.

3.2.4 Detector

An Andor Newton DU920P back illuminated CCD with a blue optimized AR coating was chosen due to its high quantum efficiency of >90% over the H&K spectrometer's bandpass, which was necessary to achieve the overall instrument throughput requirements. The 26 μm pixel size option was chosen to enable the desired 4 pixel sampling without binning and a respective 1024 by 255 pixel format that neatly fits the five spectral orders for each fiber. A wedged detector window was chosen to avoid fringing. The detector will be cooled with glycol to a temperature of -100 C in operation, but testing was performed with Thermoelectric Cooling (TEC) to -60 C.

Because the Andor exists completely enclosed in its light and dust tight box, the ambient temperature within the enclosure can quickly heat up. We found during testing on hot summer days (∼30 C lab temperatures) that the Andor would turn off the TEC to prevent damage to the system. We do not expect this issue to re-occur at Keck as we plan to cool the Andor via its integral glycol ports.

Tests with the Andor were performed to determine the optimal pre-amplifier settings and clocking speeds for operation. A pre-amp setting of 2 and a horizontal speed of 0.05 MHz resulted in a read noise of 5.8 e-, which did no vary significantly with the vertical speed. A vertical speed of 76.9 μs was chosen to maintain consistency between exposures; changes in this value also have little effect on read out time. The dark current was measured to be 0.41 e-/pixel/sec and the gain to be 5.26 e-/ADU. These values were consistent with those provided by Andor. In a pre-amp=2 setting, full well is expected to be 500,000 e-, though saturation occurs at 337,000 e- due to hitting the 16 bit limit. A linearity measurement showed that this setting was ideal for enforcing operations in a linear regime of the detector.

3.2.5 Cross Disperser

A VPH transmission grating from Wasatch Photonics[§] was chosen as the cross disperser. Since the collimated beam off the echelle passes through the VPH at a different AOI than what originally exited the VPH (a difference of 4 degrees due to the 2 degree echelle gamma angle), a symmetric VPH optimized for an AOI between the

[‡]https://www.nationalaperture.com/
[§]https://wasatchphotonics.com/

two angles incident on the VPH (11.4 degrees) was requested. The line density of 1000 lpmm was chosen to appropriately space the orders on the detector.

3.3 Tolerancing

Tolerancing of the design was performed to inform the mechanical and lens manufacturing tolerances as well as the optomechanical adjustments needed for alignment. To perform the tolerancing analysis, the sequential Zemax model was formatted following the work in Ref. 2. A min/max analysis was first performed to adjust tolerance values in order to achieve spot RMS values <26 μm (consistent with the detector pixel pitch) as a result of perturbations to each individual optic. This spot RMS limit was chosen to reflect the instrument resolution requirement of R∼16,000. A Monte Carlo sampling of all perturbations was then performed to ensure all iterations of possible combinations of alignment errors resulted in a combined error of <26 μm.

3.4 Thermal Analysis

For the expected range in temperatures to expect over the H&K spectrometer's operational lifetime, we referred to night time temperatures (4pm to 2 hours after sunrise) in the AO electronics room that were recorded for the entire year of 2016. The maximum temperature range observed over this year was 8 C to 16 C, which were used to compute the impact of temperature on the spectrometer. For this analysis, an aluminum camera barrel was considered by setting the coefficient of thermal expansion (CTE) for the space between the singlet and double camera lenses to that of standard aluminum: $23\times10^{-6}(^{\circ}C)^{-1}$. A steel optical bench and aluminum optical bench were both considered as well by applying their respective CTE values to the free space in the Zemax model. All glass components were included in the thermal analysis. Thermal pickups in the Zemax thermal configuration window were done for 8 C and 16 C temperatures, and the merit function editor was used to evaluate the spot RMS (optical quality) and spot location (image movements). The optical quality was found to be insensitive to the 8 C temperature change in consideration. The spot locations did shift however by a maximum of 0.08 pixels in the cross dispersion direction and 0.23 pixels in the dispersion direction. We can conclude from this analysis that there are no concerns the spectrum will shift vertically more than one pixel due to temperature effects. This simplifies the extraction procedure as the order traces should not need to be re-evaluated. The movements in the dispersion direction imply that the wavelength solution may need to be checked and adjusted nightly. We note that thermal simulations in Zemax are somewhat limited and these expected shifts will be checked once in operation.

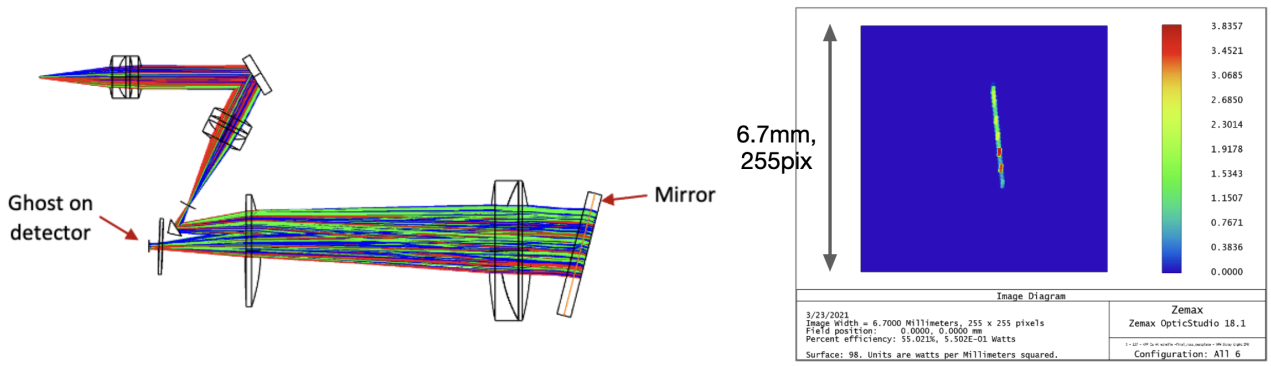

Figure 4. An example Zemax setup of the VPH ghost analysis for an transmitted ghost in orders zero then order +1 (left) and the corresponding ghost image (right). Several other order combinations produce ghosts on the same spot on the detector.

3.5 Ghost Analysis

Ghosts from the detector window and from the VPH were evaluated by setting various surfaces to mirrors and measuring the intensity of any reflected beam on the detector. A threshold value of 0.01% was adopted to judge tolerable ghost contrasts.

An internal reflection within the Andor's detector window results in a defocused ghost at a contrast of 1e-7 compared to the main beam; this number considers the window AR coating and spot defocus and is well below the threshold.

VPH ghosts were evaluated by considering light that makes its first pass through the VPH, transmits through the grating and reflects off the back surface of the VPH. This was done in Zemax by making the back surface of the VPH a mirror and tracing the reflected light path for combinations of different diffraction orders to determine which combinations land on the detector. An example of this setup is shown in the left of Figure 4, and the right panel shows the resulting ghost image. For the order combinations that created a ghost on the detector, the VPH AR coating and diffraction order efficiency values versus wavelength provided by the vendor were then used to evaluate the relative magnitude of the ghost. Since the ghosts fall in the same part of the detector, the relative throughput of each VPH was summed and found to have a total contrast of $\approx 5 \times 10^{-5}$. This was below but close to the tolerable threshhold. Steering the VPH ghost off important parts of the spectrum is possible to mitigate its impact on performance.

4. MECHANICAL DESIGN

The mechanical design of the H&K spectrometer considered the optical tolerances, alignment scenario, and how it would be stored during operations. Custom mounts were designed for the echelle, VPH, camera barrel, input relay lenses, small folder mirror near the Andor, and the Andor itself. The optical base plate was also custom made with tapped holes positioned in the correct locations for mounting the echelle mount, the camera, and the detector. The camera's position was fixed with removable shims to adjust the space between the two lenses. The VPH was also mechanically placed but attaches to the optical board with slots that constrain VPH adjustments to rotations to simplify adjustments in the VPH angle relative to the beam. The input relay optics, including the slit and the small fold mirror, were mounted on a separate plate that attaches to the main optical board with three kinematic bases and could be easily removed for alignment or access to the detector. Figure 5 shows the designs of the input relay and the custom mounts for various optics in more detail. The baffle inside the camera mount was positioned to reduce stray light reflections from reaching the Andor. Additionally, a mask was installed on the echelle mount to reject stray light outside of a cone with focal ratio f/3.5.

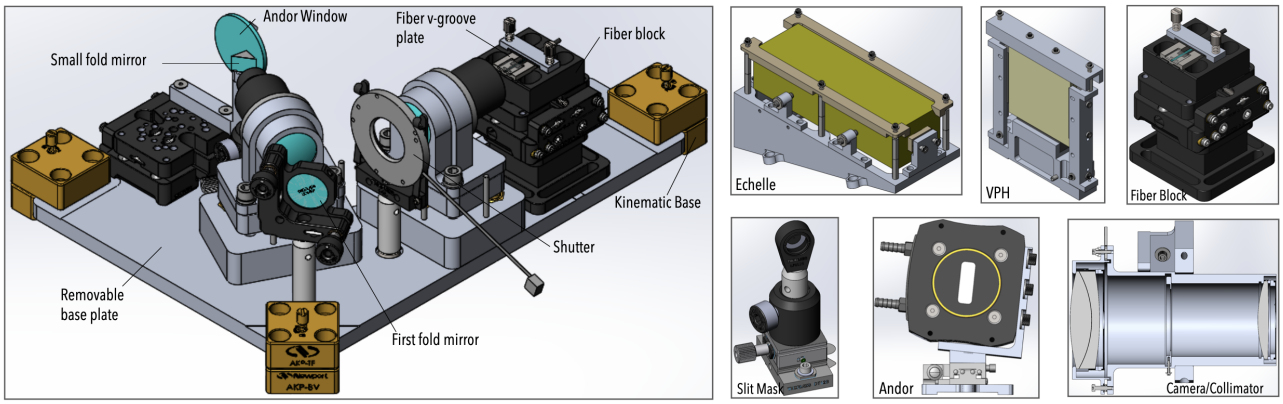

Figure 5. Mechanical drawings showing the fiber input relay (left) and select custom mounts in the instrument (right).

The optical fibers were cleaved and terminated with glass ferrules. This work was done at SSL and more details on the techniques used to terminate the fibers can be found in Ref. 12. Both fibers' focal ratio degradation (FRD) values were measured before and after bonding to the v-groove plate and, in both instances, were found to be < 0.1, corresponding to a full-cone focal ratio of >f/3.9 (97% encircled energy). To ensure light from both fibers leaves parallel to avoid relative offsets in their paths that cannot be corrected in alignment, the cleave angles of the science and sky fiber were aligned to < 0.1 deg. To ensure similar final focus positions, the fibers' relative position in focus was aligned to better than 20 μm.

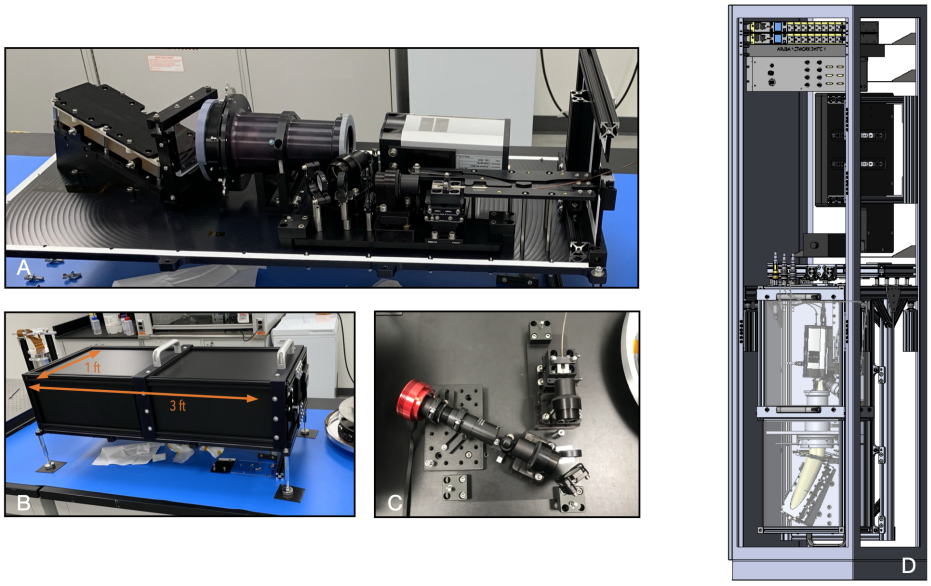

Figure 6. Images of the H&K spectrometer assembled in the lab at Caltech (left) and a drawing of the H&K spectrometer's final installation position within a rack in the AO Electronics Room on the Keck I telescope.

5. OPTICAL ALIGNMENT

The assembly of the H&K spectrometer started at UC Berkeley in spring of 2021 and was moved to Caltech in the summer to finish the assembly and begin alignment. The alignment sequence began with aligning the input relay (excluding the small second fold mirror), shown in the left of Figure 5 as well as in panel C of Figure 6. The alignment of the input relay was done using a 405 nm laser from Thorlabs that was used to illuminate the back end of the central sky fiber. Although adjustable if needed, the lens positions in the input relay were first mechanically positioned and ultimately did not need to be moved to achieve alignment. The lens mounts had SM1 threads that were used to attach temporary mirrors that, along with targets and a slit viewing camera, were used to align the input relay in the following steps:

1. The fiber was first mechanically positioned to its nominal location, then adjusted to ensure a reflected beam passed back through the first lens landed back on the fiber tip. The pupil mask (not shown in Figure 5) was also used to ensure the fiber mount was centered.

2. A mirror was attached at the back of the second lens, on the side nearest the position of the slit, in order to reflect light back through the system to the fiber. The first fold mirror was installed and adjusted such that the returned beam was centered on the central illuminated fiber.

3. A ZWO ASI120MM-S detector with a small (3.5 μm) pixel pitch, combined with a Thorlabs achromatic doublet pair with 3:1 magnification, was used to view the fiber and ensure it was in focus and aligned on the slit. The slit viewing camera was secured on the input relay plate in lieu of the small, second fold mirror, as shown in panel C of Figure 6. The slit was illuminated with low level ambient light in order to focus the slit viewing camera on the slit. With the slit viewing camera in position, the fiber was then illuminated and its focus position was adjusted to focus the fiber on the slit. The resulting aligned slit image is shown in the left panel of Figure 7.

Once the input relay was aligned, it was installed back onto the optical board. The small, second fold mirror was then adjusted followed by the VPH, echelle, then the Andor as follows:

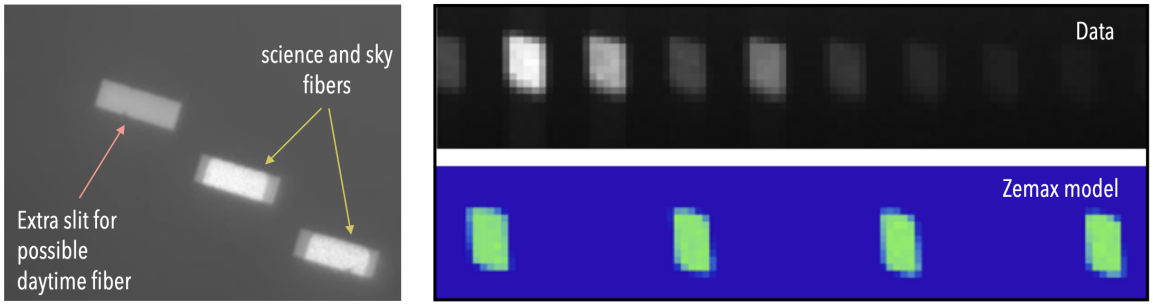

Figure 7. Fiber image aligned on the slit (left) and resolution elements of the full spectrometer compared to those of the Zemax model (right). Note that the number of resolution elements sampled in the model was not matched to the number of modes of the 405 nm laser imaged here.

1. To increase visibility, a bright green laser pointer was used to illuminate the central fiber. Zemax footprint diagrams at a small distance in front (Andor side) of the L1 singlet, and on the back (echelle side) of the L2 doublet, were printed to scale and secured to 3D printed plates that attached to the camera barrel. The small fold mirror was adjusted such that the beam was aligned with the footprint diagrams at L1 and L2.
2. The VPH was installed and adjusted such that the VPH ghost (discussed in §3.5) fell near the expected central location on the camera. Detector focus was adjusted to focus the ghost, which has the same focal distance as the spectrum.
3. A footprint of a 405 nm beam at the location of the echelle mask was printed out to scale and secured on the echelle mask. Small adjustments were made to the fold mirror such that the footprints at L1 and L2 were still aligned and remaining adjustments were applied to the echelle.
4. The echelle mask and footprint diagrams on the camera barrel were removed such that a spectral image landed on the Andor. The spectrum on the Andor was positioned to fall in the region of the detector indicated in the Zemax model. These movements were done by verifying the VPH angle positioning, and then tweaking the echelle angles.
5. The position of the Andor was moved to achieve best focus. Slight adjustments were made to the fold mirror to search for improvements to the image quality.
6. Steps 1-5 were repeated until alignment was reached as judged by comparing the resolution elements to that of the Zemax image analysis model.

There were some challenges with aligning the spectrograph, including the degeneracy between the fold mirror positions and between the echelle angles, as well as between the detector clocking and the echelle roll angle. After the first initial alignment, a noticeable tilt in the orders was observed. We chose to correct this tilt by wedging the detector mount with shims since the tolerance of the Andor mount machining process could have feasibly allowed for deviations in the observed detector clocking angle, whereas the echelle roll angle was less likely to be the culprit since it was mechanically set to the right value upon installation. This shimming process worked well to align the orders with respect to the pixel grid.

An additional challenge encountered was that removing and reinstalling the fiber v-groove plate was not repeatable to the precision required to have the fiber faces aligned to the slit upon reinstallation. This was due to some play in pushing the fiber v-groove plate against the ridged stops on the fiber mount as well as some grab by the clamping mechanism as it was tightened to hold the fiber in place. An improved fiber clamping design could alleviate this issue and also better secure the v-groove in place, but instead we mitigated the misalignment between fiber faces and the slit mask by adopting a procedure that was performed after each time the fiber v-groove plate was reinstalled in the system. This procedure was to illuminate the spectrograph with light from the 405 nm laser or emission lamp light (typically UNe) and to use the fine adjustment knob on the slit mount

to adjust the slit mask horizontally in order to maximize the light through the slit as quantified by the summed flux in a single resolved resolution element. Alternatively, though the image of the slit on the Andor is low resolution, a keen eye could discern when the fiber was aligned on the slit based on the shape of the resolution element alone. The resolution elements of the final aligned instrument is shown in the right panel of Figure 7, in which model images of the resolution element generated using the Geometric Image Analysis tool in Zemax are also shown for comparison.

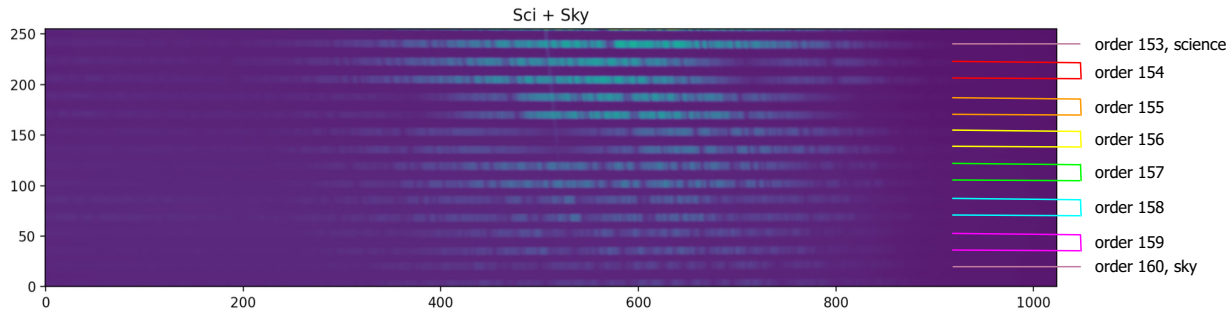

Figure 8. Echellogram showing solar observations taken with the H&K spectrometer. Science and sky fibers were illuminated separately then co-added in software to produced this image. The final positioning of the spectra will be adjusted in the instrument's final alignment at WMKO such that order 153 of the sky fiber is positioned onto the detector at the expense of order 160.

6. DESIGN PERFORMANCE AND VERIFICATION

The H&K spectrometer was moved to Berkeley in April 2022 for integration and testing with the main spectrograph. The instrument was realigned and set up in a space in the high bay of the Space Sciences Laboratory (SSL) building, which allowed for somewhat clean conditions to open the enclosure to install the fibers, but suffered from light leaks during the day time testing. The instrument was injected with solar light and calibration light to derive a wavelength solution, measure the spectral format, and validate the resolution across the spectrum. A sequence of solar data were also analyzed to monitor wavelength drifts and extract a series of S_{HK} indices.

The solar light was injected using the KPF Solar Calibrator (SoCal), which utilizes an off-the-shelf solar tracker that was placed on top of the Space Sciences Laboratory building and focused solar light into an integrating sphere that coupled into a fiber that was routed to the lab. An echellogram of the solar spectrum illuminating both sky and science fibers (imaged separately then co-added) is shown in Figure 8. It can be seen in Figure 8 that the science trace in order 153 has no sky counterpart. This alignment error is related to difficulties in using the 405 nm laser to center the spectrum since it only hits the detector in order 152, which is outside the H&K spectrometer's bandpass. The manufactured echelle blaze angle also slightly differs from the specified blaze angle, which changes the wavelength bounds of each order compared to that of the model. The blaze angle was re-measured using the central peaks in the flat field spectrum plotted in gray in Figure 9 and was found to be 75.5 deg, which is slightly lower than that of an R4 (75.96 deg). At summit during final realignment, a UNe lamp will be used, which will allow for an easier job of positioning the orders on the detector.

Each dataset was dark subtracted and then a simple column sum was performed to extract 1D spectra from all the exposures. The wavelength solution was found by fitting the H&K UNe spectra to the NEID UNe spectrum and solving for the Legendre coefficients that map pixels to wavelength space; the coefficients were initialized with the approximate dispersion and midpoint wavelength of each order. Figure 9 shows the extracted solar spectrum for the science fiber trace. Plotted over the solar spectrum is an extracted flat lamp spectrum shown in gray. Both spectra were normalized by the maximum flux value in each order; the spikes in the gray spectra show the position VPH ghost. In the test setup, the ghost overlaps near the core of the K line and in adjacent orders used for the comparison continuum regions. In the final alignment, the VPH angle and possibly also the echelle tilt (blaze direction) will be adjusted to move this ghost off important regions of the spectra.

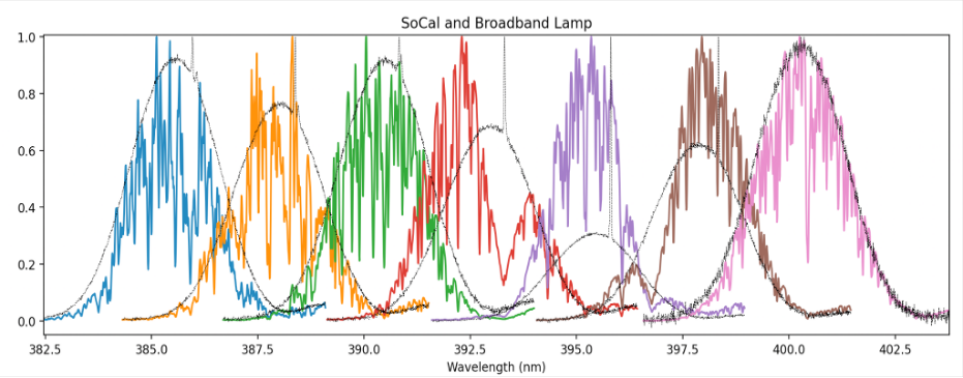

Figure 9. Extracted solar spectra from the science trace of the H&K spectrometer shown as the colored lines and a flat field spectrum plotted in gray. Both spectra have been normalized to a peak flux of 1. Order 159 is in blue on the left and order 153 is in pink on the right.

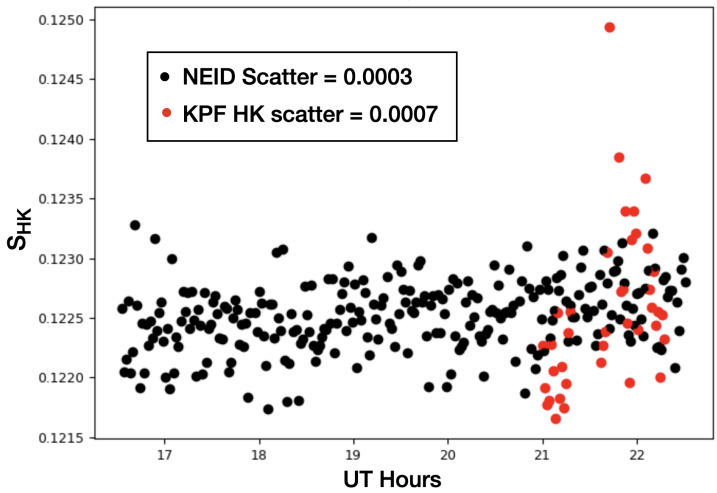

Figure 10. S_{HK} indices derived from a sequence of solar observations with the H&K spectrometer on April 29th, 2022 (UT) compared to NEID S_{HK} indices.

A basic extraction of the S_{HK} values was performed on solar data taken on April 29th, 2022 (UT) using approximately 2 Å regions centered around the H and K lines and continuum references from 399 nm to 401 nm and 389 nm to 391 nm. NEID S_{HK} values were downloaded for this day and the H&K spectrometer values were shifted to overlap the NEID values for a relative comparison, shown in Figure 10. The red points of the H&K show a larger RMS (0.0007) compared to NEID (0.0003), but still below the goal of $S_{HK} < 0.001$). It should be noted that S_{HK} showed measurable correlation with both spectral SNR and dark current, implying poor dark subtraction and possible effects due to the VPH ghost causing added scatter in the H&K spectrometer S_{HK} values. We therefore expect that in its final operating condition with an improved VPH ghost position, a nighttime environment with a more stable dark flux, and a more careful extraction that takes into accounts velocity shifts should further improve the performance of the H&K spectrometer.

7. CONCLUSIONS

The Ca II H&K lines serve an important role in validating new exoplanet discoveries made with radial velocity spectrographs. The flux in the cores of the lines trace chromospheric activity in the star and can serve as a tracer for radial velocity signals that are due to the host star and not a planet. Spectrographs like the Keck

Planet Finder whose wavelength coverage does not overlap the Ca II H&K lines may choose to build a separate instrument dedicated to measuring the Ca II H&K activity index. In this work we detailed the design of KPF's dedicated Ca II H&K spectrograph that will operate simultaneously with the main spectrometer. KPF's H&K spectrometer has a double pass, cross-dispersed echelle design and covers 393 nm-403 nm at a resolving power of 16,000 and expected throughput of 4-7%. In July the H&K spectrometer was shipped to Hawaii. In August of 2022 it will be unpacked at Keck Observatory, realigned, then installed in the AO room of Keck I, where it will be fed light from KPF's fiber injection unit. Commissioning of KPF along with the H&K spectrometer is expected to happen in late fall of 2022.

ACKNOWLEDGMENTS

The authors would like to thank the Jet Propulsion Lab, the National Science Foundation, and the Heising-Simons Foundation (HSF) for supporting this project. This work was performed in part by A.D.B. who was supported by an 51 Pegasi b Postdoctoral Fellowship funded by the HSF. We also thank Hector Rodriguez for his help setting up the lab space at Caltech, Scott Lilley at WMKO for sharing the triplet lens design and ordering those lenses. The research was carried out, in part, at the Jet Propulsion Laboratory, California Institute of Technology, under a contract with the National Aeronautics and Space Administration (80NM0018D0004)

REFERENCES

[1] Gibson, S. R., Howard, A. W., Roy, A., Smith, C., Halverson, S., Edelstein, J., Kassis, M., Wishnow, E. H., Raffanti, M., Allen, S., Chin, J., Coutts, D., Cowley, D., Curtis, J., Deich, W., Feger, T., Finstad, D., Gurevich, Y., Ishikawa, Y., James, E., Jhoti, E., Lanclos, K., Lilley, S., Miller, T., Milner, S., Payne, T., Rider, K., Rockosi, C., Sandford, D., Schwab, C., Seifahrt, A., Sirk, M. M., Smith, R., Stuermer, J., Weisfeiler, M., Wilcox, M., Vandenberg, A., and Wizinowich, P., "Keck Planet Finder: preliminary design," in [*Ground-based and Airborne Instrumentation for Astronomy VII*], Evans, C. J., Simard, L., and Takami, H., eds., **10702**, 1778 – 1797, International Society for Optics and Photonics, SPIE (2018).

[2] Gibson, S. R., "Tolerancing a radial velocity spectrometer within Zemax," in [*Modeling, Systems Engineering, and Project Management for Astronomy VI*], Angeli, G. Z. and Dierickx, P., eds., *Society of Photo-Optical Instrumentation Engineers (SPIE) Conference Series* **9911**, 99112C (Aug. 2016).

[3] Robertson, P., Mahadevan, S., Endl, M., and Roy, A., "Stellar activity masquerading as planets in the habitable zone of the M dwarf Gliese 581," *Science* **345**, 440–444 (July 2014).

[4] Fulton, B. J., Weiss, L. M., Sinukoff, E., Isaacson, H., Howard, A. W., Marcy, G. W., Henry, G. W., Holden, B. P., and Kibrick, R. I., "THREE SUPER-EARTHS ORBITING HD 7924," *The Astrophysical Journal* **805**, 175 (jun 2015).

[5] Meunier, N., "Stellar variability in radial velocity," *arXiv e-prints* , arXiv:2104.06072 (Apr. 2021).

[6] Robertson, P., Bender, C., Mahadevan, S., Roy, A., and Ramsey, L. W., "Proxima Centauri as a Benchmark for Stellar Activity Indicators in the Near-infrared," **832**, 112 (Dec. 2016).

[7] Wilson, O. C., "Flux Measurements at the Centers of Stellar H- and K-Lines," *apj* **153**, 221 (July 1968).

[8] Isaacson, H. and Fischer, D., "CHROMOSPHERIC ACTIVITY AND JITTER MEASUREMENTS FOR 2630 STARS ON THE CALIFORNIA PLANET SEARCH," *The Astrophysical Journal* **725**, 875–885 (nov 2010).

[9] Vogt, S. S. and Donald Penrod, G., "Hires: A high resolution echelle spectrometer for the keck 10-meter telescope," in [*Instrumentation for Ground-Based Optical Astronomy*], Robinson, L. B., ed., 68–103, Springer New York, New York, NY (1988).

[10] Lilley, S., Rider, K., Thorne, J., Kassis, M., Gibson, S., Howard, A., Lanclos, K., and Walawender, J., "A fiber injection unit for the Keck Planet Finder: opto-mechanical design," Ground-based and Airborne Instrumentation for Astronomy, SPIE (2022).

[11] Magrath, B., "Reflectivity Degradation Rates of Aluminum Coatings at the CFHT," *pasp* **109**, 303–306 (Mar. 1997).

[12] Sharon Jelinsky, Martin M. Sirk, C. P. in prep (2022).